Identifying mechanistic differences between co-fed CO_2 hydrogenation and reactive CO_2 capture using Ru and Pd dual function materials

Chae Jeong-Potter[†,]*, Neha Mehra, Carrie A. Farberow, Daniel A. Ruddy*

National Laboratory of the Rockies, Catalytic Carbon Transformation and Scale-Up Center, Golden, Colorado, 80401, USA

**Corresponding authors: Chae Jeong-Potter,* cjeongpo@syr.edu*; Daniel Ruddy,* dan.ruddy@nlr.gov

[†]Present address: *Department of Biomedical and Chemical Engineering, Syracuse University, Syracuse, New York, 13244, USA*

Supplementary Figures

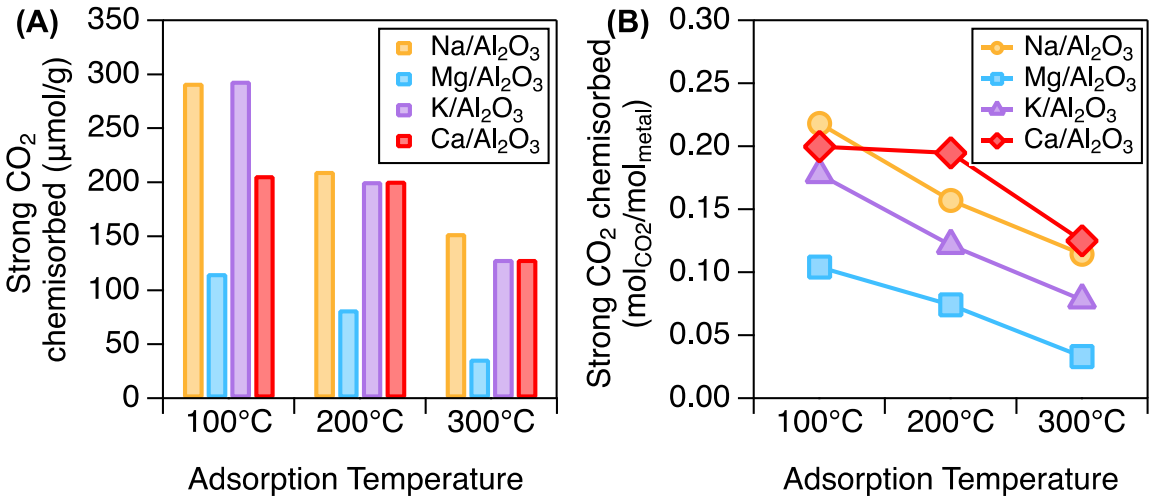

Figure S1: (a) Strong CO_2 chemisorption in µmol/g for Na/Al_2O_3 (yellow), Mg/Al_2O_3 (blue), K/Al_2O_3 (purple), and Ca/Al_2O_3 (red) over a range of adsorption temperatures (100 °C – 300 °C). (b) Strong CO_2 chemisorption as standardized to mole of sorbent metal. Samples were thermally treated in N_2 at 400 °C for 4 h, followed by an 8 h evacuation before analysis.

Supplementary Note: The analysis temperatures in **Figure S1** above were chosen to represent capture over a range of known power plant flue gas temperatures (e.g., 100 °C for combined cycle flue gas to 300 °C for post selective catalytic reduction (SCR) technology) and typical RCC process conditions (e.g., 200 – 400 °C). At low temperature (100 °C), G1-Alks (Na and K) offered the greatest mass-normalized strong CO_2 capacity, Ca/Al_2O_3 had a moderate capacity, and Mg/Al_2O_3 exhibited the lowest capacity. High adsorption temperature (300 °C) reduced the capacity on Mg/Al_2O_3 to just 36.8 µmol/g, and overall, the adsorption capacity for Mg/Al_2O_3 was poor throughout the range of adsorption temperatures. G1-Alks maintained moderate capacity values with Na/Al_2O_3 exhibiting 52% of its 100 °C capacity at 300 °C (153 µmol/g) and K/Al_2O_3 retaining 44% (129 µmol/g). Ca/Al_2O_3 was the least affected by increasing adsorption temperature. **Figure S1b** presents the CO_2 adsorption values standardized to the Alk molar loading.

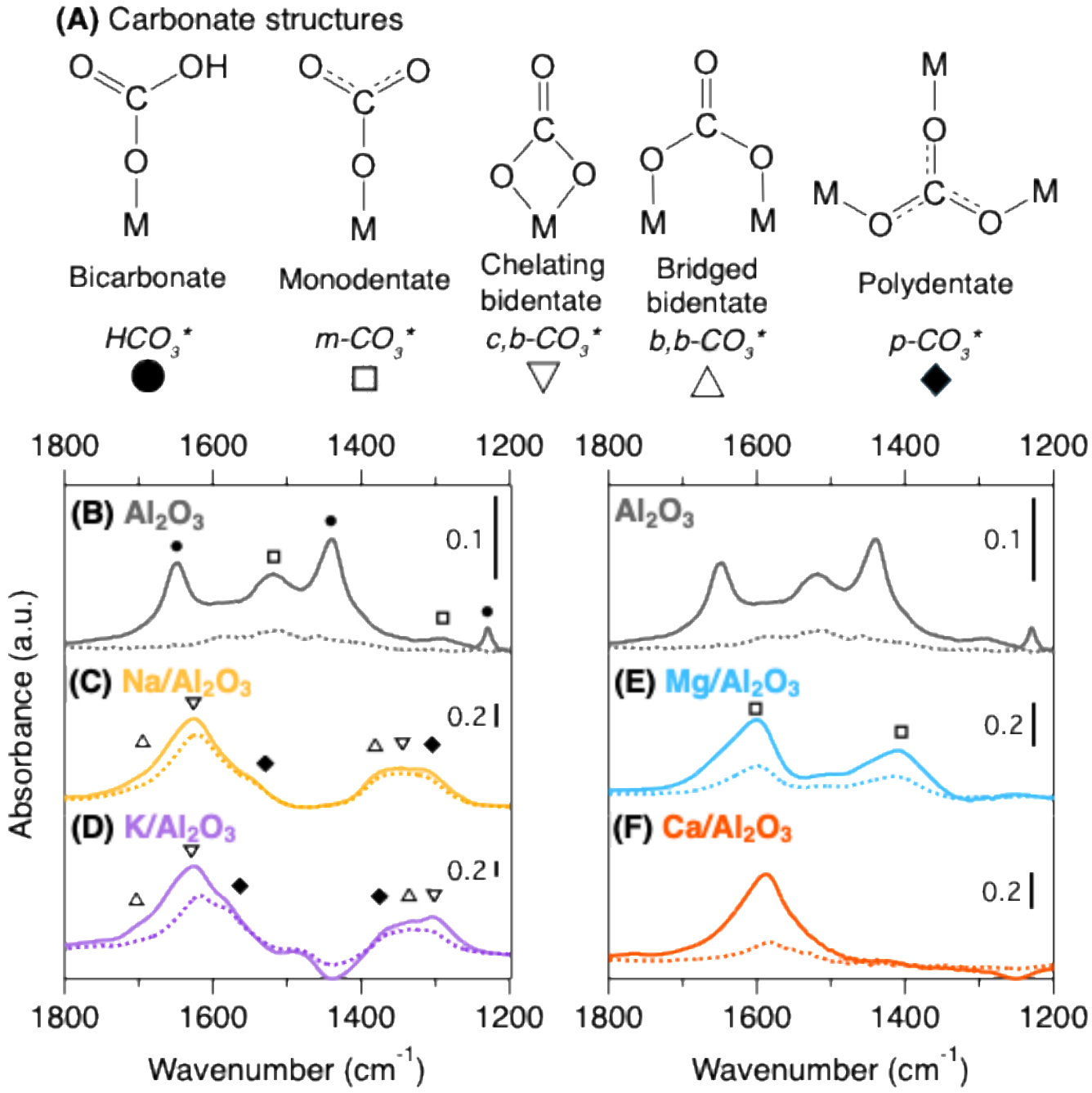

Figure S2: (a) Structures of surface carbonates assigned to the observed in situ DRIFTS spectra of (b) Al_2O_3, (c) Na/Al_2O_3, (d) K/Al_2O_3, (e) Mg/Al_2O_3, and (f) Ca/Al_2O_3 after thermal treatment with He at 300 °C for 4 h, 30 min adsorption with 5% CO_2/He at 300 °C (solid), and 30 min purge with He (dotted).

Supplementary Note: The spectra of Alk/Al_2O_3 sorbents did not exhibit any clear evidence of Al_2O_3-associated surface species, indicating that the alkali adsorptions sites dominate the interactions with CO_2. G1-Alks (Na, K) appear here to adsorb CO_2 in diverse geometries, including chelating and bridged bidentate and polydentate geometries. The G2-Alks (Mg, Ca) exhibited less diversity in binding geometries, limited to monodentate species.

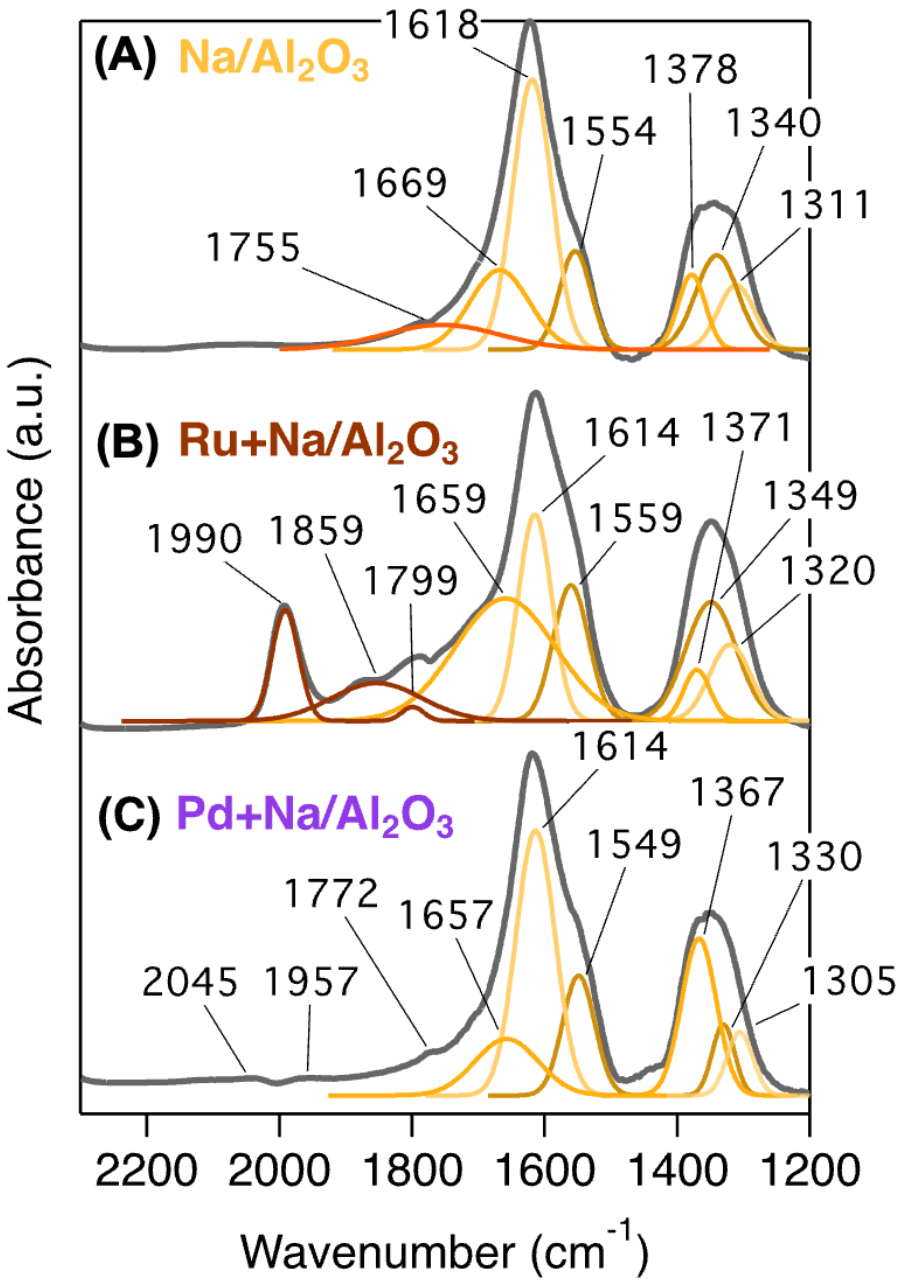

Figure S3: Large format version of Fig. 2 in main text.

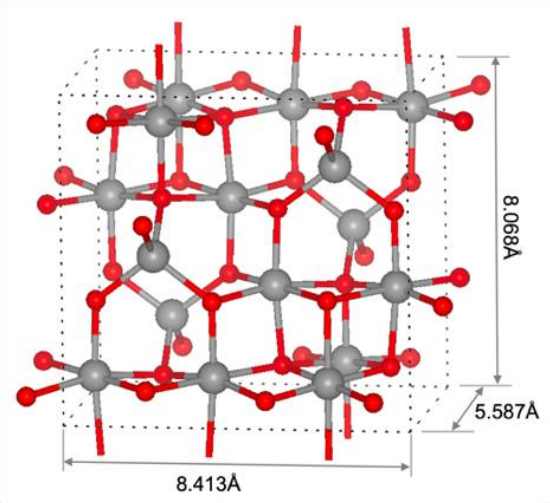

Figure S4: Optimized bulk structure of γ-Al_2O_3. Atom colors: O-red, Al-grey.

Supplementary Note: The bulk structure of non-spinel γ-alumina (γ-Al_2O_3) was obtained based on models constructed by Digne *et al.* and Krokidis *et al.*[1,2] The structure is depicted in **Figure S4**. The PBE-computed lattice constants of a periodic model containing 8 Al_2O_3 units, obtained through a structural optimization using 3 × 2 × 2 k-point mesh, are a = 5.587 Å, b = 8.413 Å, c = 8.068 Å, in good agreement with the prior reports.

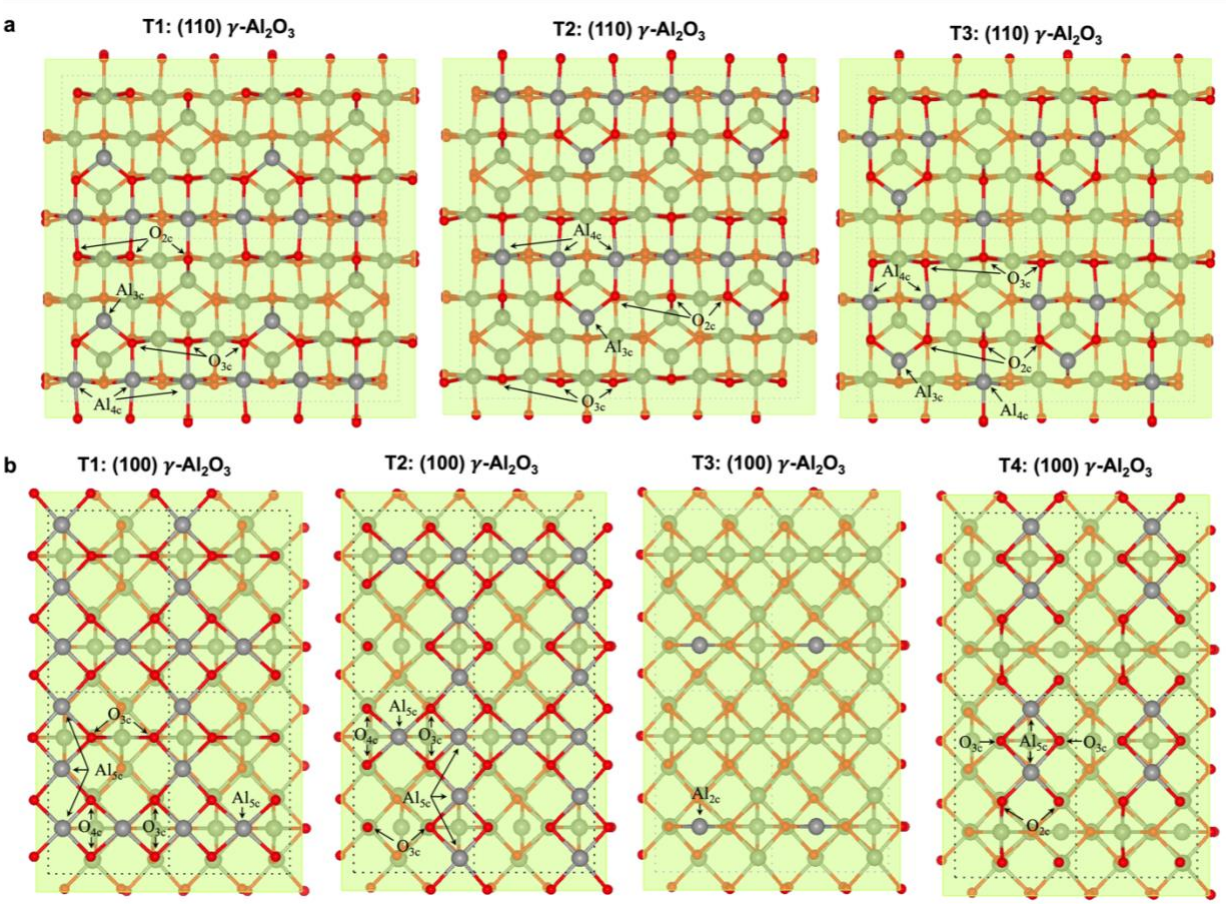

Figure S5: Top view of unrelaxed, as-cleaved terminations of the (a) (110) and (b) (100) surfaces of γ-Al_2O_3. Atom colors: O-red, Al-grey.

Supplementary Note: Four-layer (4L) slabs of the (110) and (100) surfaces were cleaved from bulk γ-Al_2O_3. The (110) and (100) facets are chosen based on prior reports of the dominant surfaces of γ-Al_2O_3.[1] The cleavage and surface energies (σ) of various surface terminations (**Table S2**) were computed for the unrelaxed (shown in **Figure S5**) and relaxed periodic slabs, respectively as

$$\sigma = \frac{1}{2A}\left(E_{slab,j} - \frac{N_{slab}}{N_{bulk}}E_{bulk}\right) \qquad \text{eq. S1}$$

where $E_{slab,j}$ is the energy of the relaxed ($j = r$) or unrelaxed slab ($j = u$) in surface and cleavage energy calculations, respectively, E_{bulk} is the total energy of the bulk unit cell, N_{slab} is the number of atoms in the slab unit cell, N_{bulk} is the number of atoms in the bulk unit cell, and A is area of the surface plane in the slab unit cell normal to the z-direction in which a vacuum of 10-12 Å is applied. Eight-layer (8L) slabs for the (110) surfaces were also evaluated to compare with values previously reported by Digne *et al.,* resulting in good agreement with the prior report.[1]

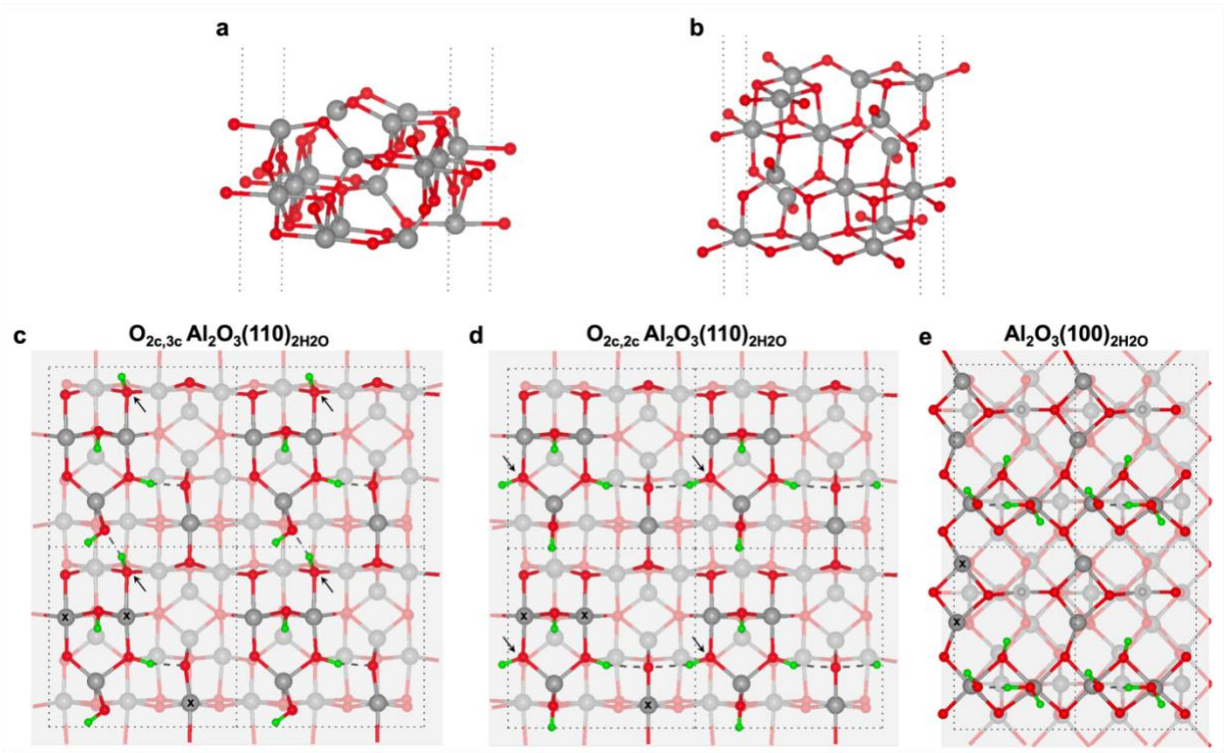

Figure S6: Side view of relaxed γ-Al_2O_3 (a) (110) and (b) (100) surface slab models. Top view of hydrated (c) $O_{2c,3c}$ $Al_2O_3(110)_{2H2O}$ (d) $O_{2c,2c}$ $Al_2O_3(110)_{2H2O}$ and (e) $Al_2O_3(100)_{2H2O}$ surfaces. Arrows indicate the surface oxygen to which hydrogen (H) binds differently in (c) compared to (d). Black dotted lines indicate the periodic 1x1 unit cell. cus-Al are indicated by 'x'. Atoms colors: O-red, Al-grey, and H-green.

Supplementary Note: The lowest surface energy T3 termination of the relaxed (110) surface exposes 3- and 4-fold coordinated aluminum atoms (Al_{3c}, Al_{4c}) and 2- and 3-fold coordinated oxygen (O_{2c}, O_{3c}) atoms (**Figure S6a**), while the lowest surface energy T1 termination of the (100) facet is composed of 5-fold coordinated aluminum atoms (Al_{5c}) and O_{3c} in the top surface layer (**Figure S6b**). The hydrated (110) alumina surface was formed by dissociative adsorption of two water molecules, each generating one hydroxide (OH) and one hydrogen (H) bound at an exposed surface O, yielding 5.9 OH/nm^2. One water molecule dissociates across Al_{3c} and the neighboring O_{2c} to form an Al_{4c}-OH and O_{3c}-H pair. An additional water molecule can generate an OH coordinated to two Al_{4c} forming Al_{5c}-μ(OH)-Al_{5c}, while the H can bind to either the neighboring O_{3c} or O_{2c} as indicated by arrows in **Figure S6c,d** and labelled as $O_{2c,3c}$ or $O_{2c,2c}$, respectively. In 1x1 unit cell, the $O_{2c,2c}$ $Al_2O_3(110)_{2H2O}$ is more stable than $O_{2c,3c}$ $Al_2O_3(110)_{2H2O}$ by 0.15 eV, and we note that it is distinct from adsorbed structures reported previously by Digne *et al.* and Wischert *et al.*[1,3] All subsequent simulations of hydrated $Al_2O_3(110)$ utilize this $O_{2c,2c}$ surface model and are referred to as $Al_2O_3(110)_{2H2O}$. Similarly, two water molecules were adsorbed on γ-Al_2O_3 (100); on this surface the most stable structure includes one dissociated water and one molecularly bound water molecule, yielding 8.8 OH/nm^2. The optimized $Al_2O_3(100)_{2H2O}$ surface is shown in **Figure S6e** and is similar to that reported by Digne *et al.*[1] Coordinatively unsaturated aluminum (cus-Al) present on both the surfaces are indicated in **Figure S6c-e**.

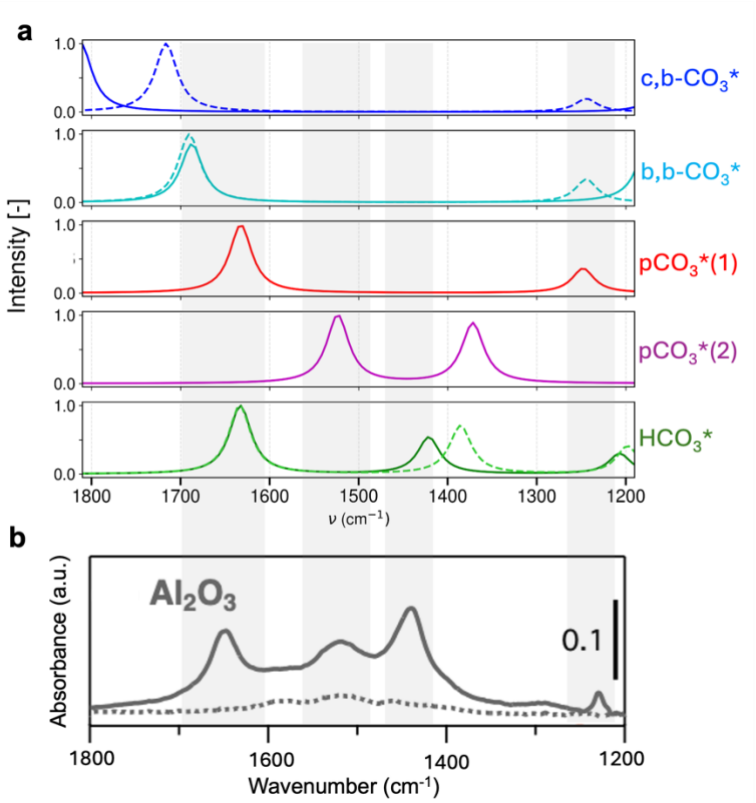

Figure S7: (a) Computed vibrational spectra of adsorbed carbonate (CO_3*) and bicarbonate (HCO_3*) on $Al_2O_3(110)_{2H2O}$ (solid lines) and $Al_2O_3(100)_{2H2O}$ (dashed lines). (b) Experimental DRIFTS spectra of CO_2 adsorption on Al_2O_3 (pre-treated with He at 300°C for 4 h, 30 min adsorption with 5% CO_2/He at 300°C (solid), and 30 min purge with He (dotted)).

Supplementary Note: Various geometries of adsorbed CO_2 on $Al_2O_3(110)_{2H2O}$ and $Al_2O_3(100)_{2H2O}$ were optimized to locate distinct adsorption configurations which have been previously categorized as: (i) physisorbed CO_2, (ii) monodentate carbonate (m-CO_3*), (iii) chelating bidentate carbonate (c,b-CO_3*), (iv) bridged bidentate carbonate (b,b-CO_3*), (v) polydentate carbonate (p-CO_3*), and (vi) bicarbonate (HCO_3*) as shown in **Figure S2**.[4–8] The optimized structures, binding energies (E_{ads}), and computed vibrational wavenumbers for all configurations are reported in **Table S3**. Physisorbed CO_2 retained a nearly linear geometry and similar bond lengths and vibrational wavenumbers as gas-phase CO_2. Computed carbonate species (ii-v) exhibited complex bound states making it difficult to assign to the specific CO_3* configurations defined in prior reports. [4–8] All structures initialized as m-CO_3* relaxed to more coordinated final configurations, indicating that monodentate carbonate configurations are unstable. Computed bidentate (c,b-CO_3* and b,b-CO_3*) structures exhibited a υ(C=O) band at higher wavenumbers (by 30-155 cm^{-1}) than the 1657 cm^{-1} peak in the experimental spectra shown in **Figure S2b**. The polydentate structure, p-CO_3*(1) showed a band near the experimentally observed peak at 1657 cm^{-1}, while a slightly different polydentate structure, p-CO_3*(2), exhibited bands near the experimentally observed peaks at 1530 and 1300 cm^{-1}. HCO_3* motifs bridged across two Al atoms exhibited computed bands at wavenumbers similar to the experimentally observed peaks (Figure S2b) at 1657, 1442 and 1230 cm^{-1} peaks and previously reported characteristic bicarbonate bands.[5–7] A comparison of the computed spectra for each CO_3* and HCO_3* motif on $Al_2O_3(110)_{2H2O}$ and $Al_2O_3(100)_{2H2O}$ surfaces with DRIFTS spectra of CO_2 adsorption on Al_2O_3 recorded at 300 °C (**Figure S2b**) is shown in **Figure S7**. As mentioned above,

bands of HCO_3* show a noteworthy overlap with the experimental peaks. There is also overlap between the experimental spectra and the simulated spectra for p-CO_3*, as well as b,b-CO_3*, although to a lesser extent. Based on the calculated energies, c,b-CO_3*, b,b-CO_3* and HCO_3* are more stable than p-CO_3* on $Al_2O_3(110)_{2H2O}$ and $Al_2O_3(100)_{2H2O}$ surfaces. Surface hydroxylation will influence the relative populations of these species as b,b/c,b/p-CO_3* are stabilized by cus-Al atoms while HCO_3* requires insertion into Al-OHs.

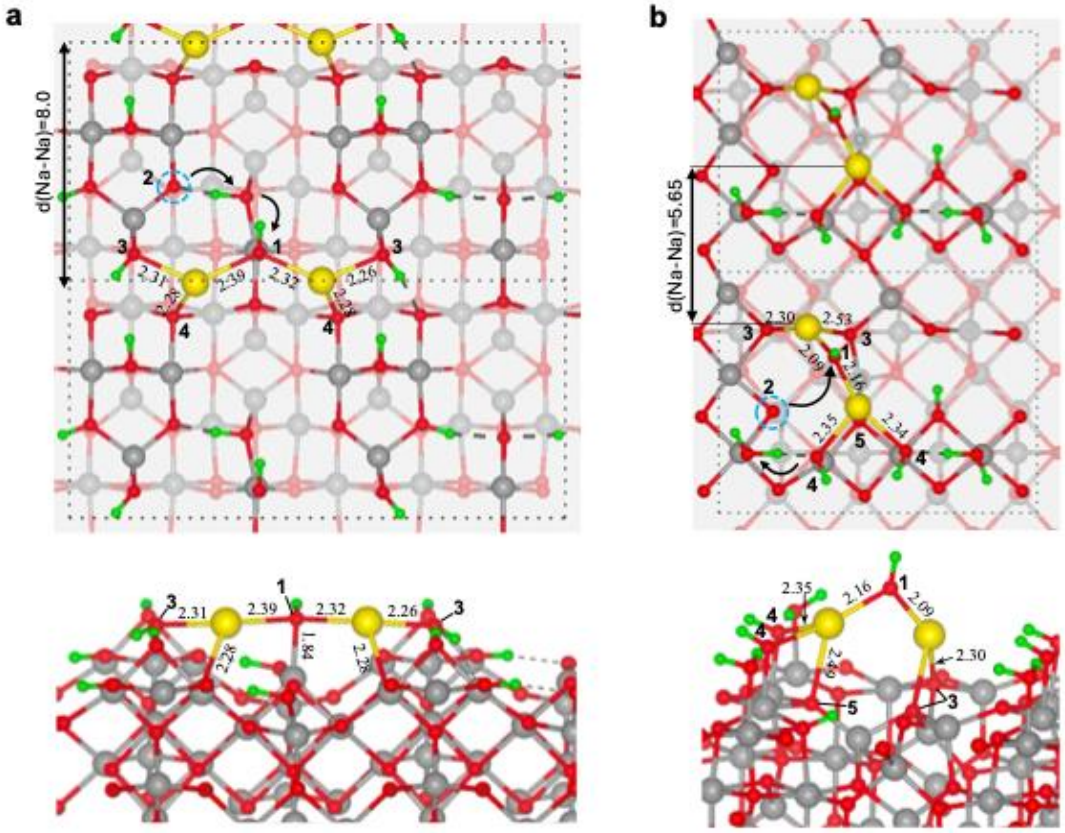

Figure S8: Top and side view of optimized Na_2O on (a) $Al_2O_3(110)_{2H2O}$ and (b) $Al_2O_3(100)_{2H2O}$. A H atom migrates from surface O (blue circle, site 2) to form [(Na_2O)H] (site 1). Black dotted lines indicate the periodic supercell. Atom colors: O-red, Al-grey, Na-yellow, and H-green. Distances in Å.

Supplementary Note: To simulate Na-modified Al_2O_3, Na_2O was added to a 2 × 1 supercell of $Al_2O_3(110)_{2H2O}$ and $Al_2O_3(100)_{2H2O}$. Multiple Na_2O binding configurations were evaluated such that the oxygen atom of Na_2O (**Figure S8**, site 1) coordinated to one of the cus-Al sites, the most stable of which are depicted in **Figure S8**. Migration of a surface H from an adjacent Al-OH (**Figure S8**, site 2) to Na_2O (**Figure S8**, site 1) resulted in [(Na_2O)H] species. The other surface O sites coordinated to Na atoms are numbered as 3-5 in **Figure S8**. The Na coverage on the $Al_2O_3(110)_{2H2O}$ and $Al_2O_3(100)_{2H2O}$ model surface is 1.47 Na/nm^2 and 2.13 Na/nm^2, respectively. Correspondingly, Na are separated by a larger distance on $Al_2O_3(110)_{2H2O}$ than on $Al_2O_3(100)_{2H2O}$ as indicated by d(Na-Na) in **Figure S8**.

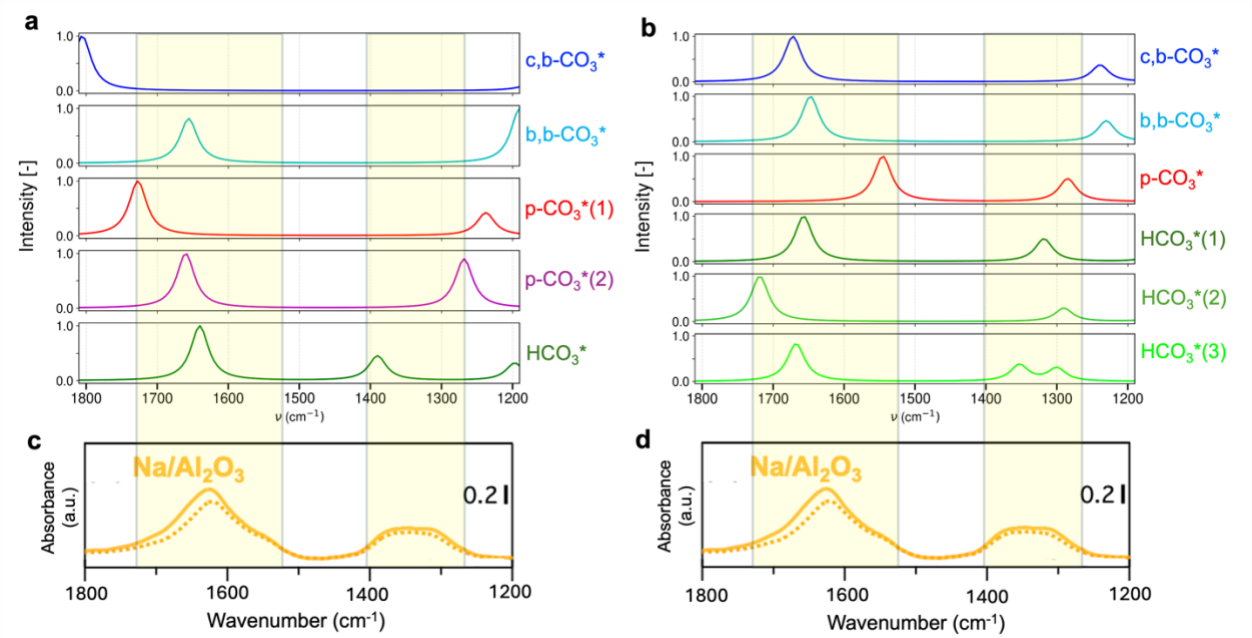

Figure S9: Computed vibrational spectra of adsorbed carbonate (CO_3*) and bicarbonate (HCO_3*) on (a) $Na/Al_2O_3(110)_{2H2O}$ and (b) $Na/Al_2O_3(100)_{2H2O}$. c) and d) Experimental DRIFTS spectra of CO_2 adsorption on Na/Al_2O_3 (pre-treated with He at 300°C for 4 h, 30 min adsorption with 5% CO_2/He at 300°C (solid), and 30 min purge with He (dotted)).

Supplementary Note: Several stable adsorbed structures for physisorbed CO_2, c,b-CO_3*, b,b-CO_3*, p-CO_3* and HCO_3* were identified on Na-modified $Al_2O_3(110)_{2H2O}$ and $Al_2O_3(100)_{2H2O}$ surfaces (referred to in the text that follows as $Na/Al_2O_3(110)_{2H2O}$ and $Na/Al_2O_3(100)_{2H2O}$, respectively). The most stable structures on both Al_2O_3 surface models, reported in **Table S4,** indicate that b,b- and p-CO_3* adsorb coordinated to Na and Al atoms whereas c,b-CO_3* coordinates only to Al. Stable HCO_3* structures were identified coordinated to Na (**Table S4**, HCO_3*(1-3)) or to both Na and Al (**Table S4**, HCO_3*(4)) on $Na/Al_2O_3(100)_{2H2O}$. On $Na/Al_2O_3(110)_{2H2O}$, all stable HCO_3* structures were coordinated to both Na and Al. HCO_3* structures (1-3) on $Na/Al_2O_3(100)_{2H2O}$ exhibit a mix of chelating, bridged and H-bonding conformations. The computed vibrational wavenumbers of all CO_3* and HCO_3* structures located on Na/Al_2O_3 surfaces are provided alongside the experimental DRIFTS spectra in **Figure S9**. While there are some computed bands for bidentate (b,b/c,b-CO_3*) and polydentate (p-CO_3*) carbonates that overlap with the experimental spectra, HCO_3*(1-3) coordinated to Na atoms on $Na/Al_2O_3(100)_{2H2O}$ showed the most significant overlap with the experimental spectra. The computed wavenumbers are notably distinct from HCO_3* adsorbed on Al_2O_3 (**Table S3**) and HCO_3*(4) bound across Na and Al binding sites on $Na/Al_2O_3(100)_{2H2O}$ (**Table S4**).

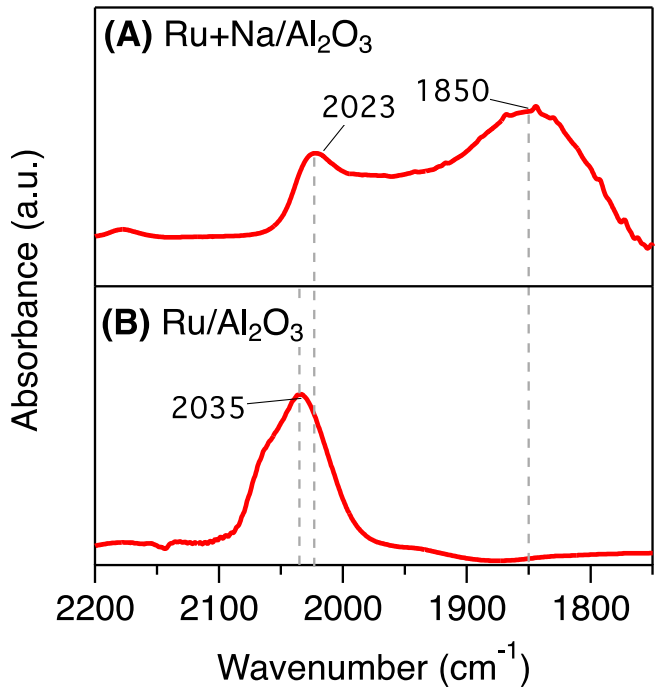

Figure S10: *In situ* DRIFTS spectra of CO adsorption at 300°C on (a) Ru+Na/Al_2O_3 DFM and (b) Na-free Ru/Al_2O_3 catalyst.

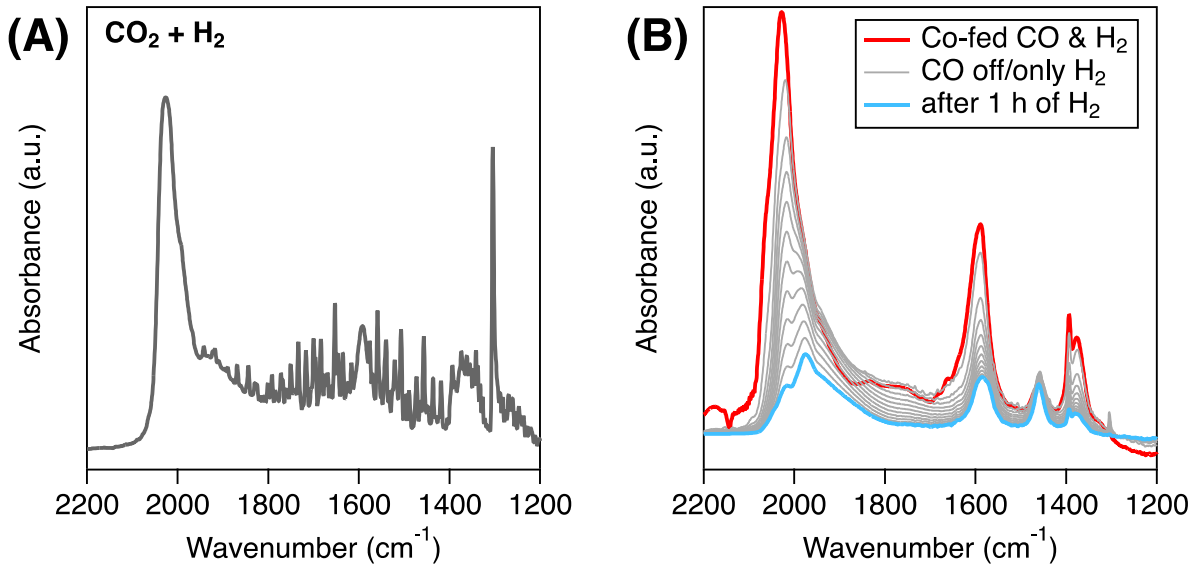

Figure S11: In situ DRIFTS spectra of (a) co-fed hydrogenation of CO_2 (CO_2:H_2 = 1:4, 10% CO_2,40% H_2, balance He) and (b) co-fed hydrogenation of CO (CO:H_2 = 1:3, 10% CO, 30% H_2, balance He) over Ru/Al_2O_3 at 300 °C.

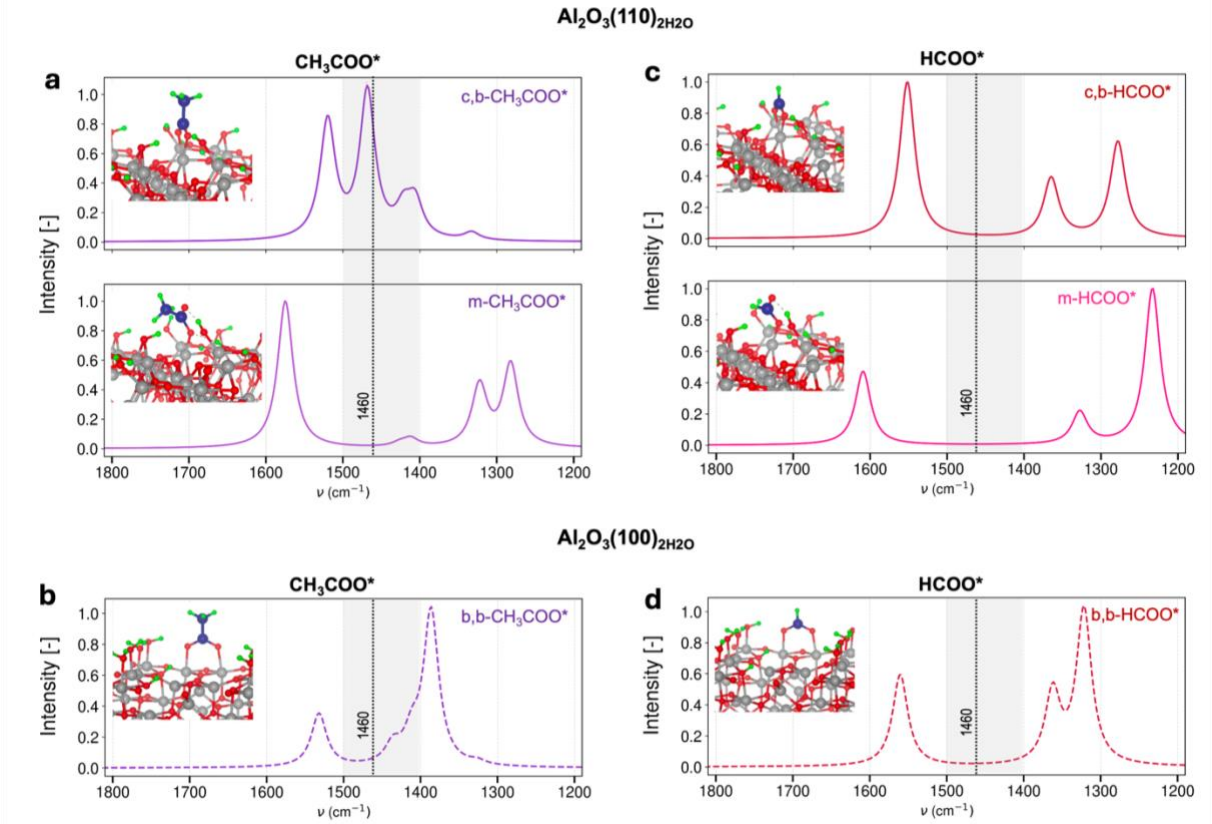

Figure S12: Computed vibrational spectra of adsorbed acetate (CH_3COO^*) on (a) $Al_2O_3(110)_{2H2O}$ and (b) $Al_2O_3(100)_{2H2O}$ and formate ($HCOO^*$) on (c) $Al_2O_3(110)_{2H2O}$ and (d) $Al_2O_3(100)_{2H2O}$. Atom colors: O-red, Al-grey, H-green, C-dark blue.

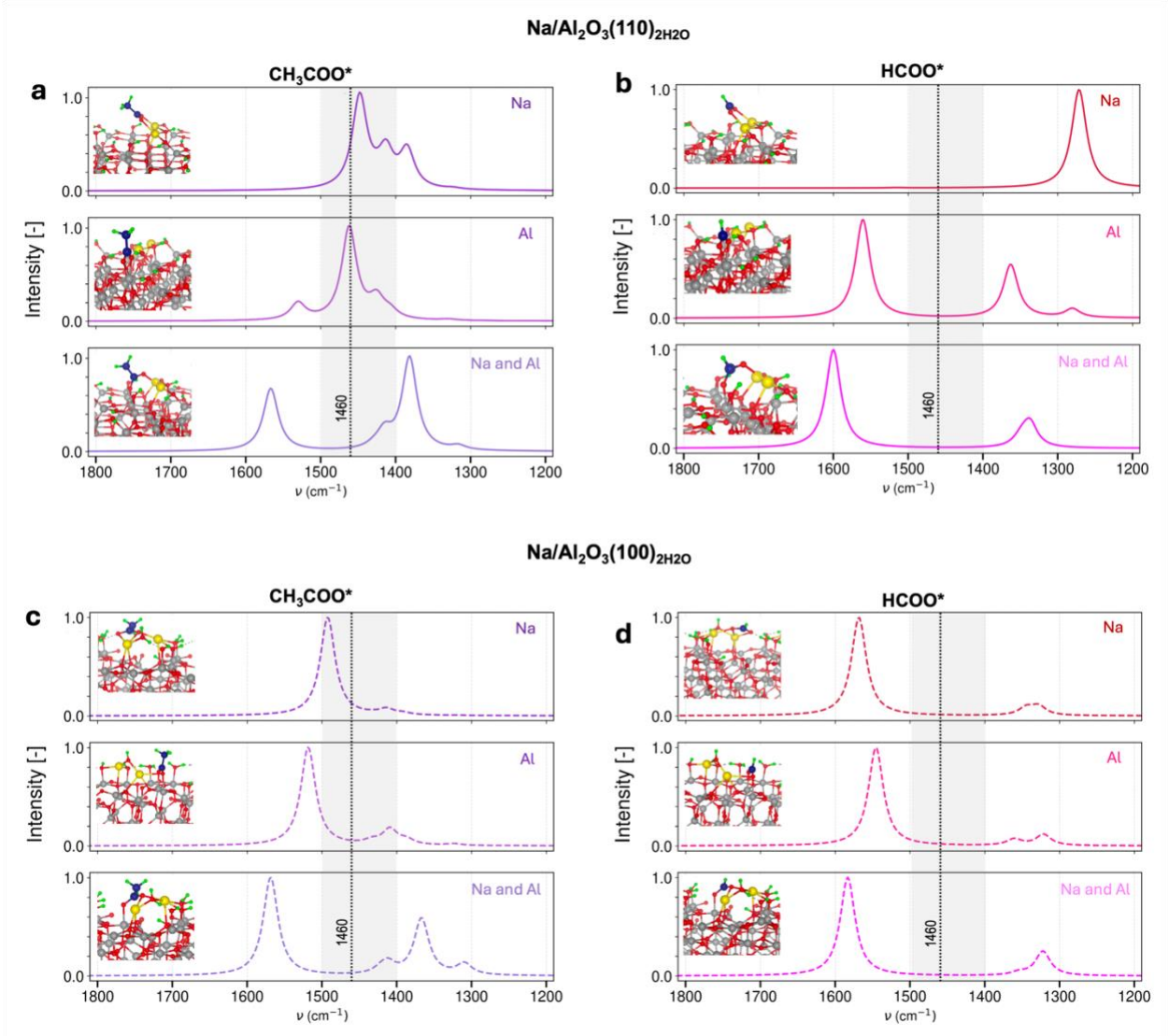

Figure S13: Computed vibrational spectra of bidentate adsorbed acetate (CH_3COO^*) on Na-modified (a) $Al_2O_3(110)_{2H2O}$ and (c) $Al_2O_3(100)_{2H2O}$ and bidentate formate ($HCOO^*$) on Na-modified (b) $Al_2O_3(110)_{2H2O}$ and (d) $Al_2O_3(100)_{2H2O}$. The elements to which the adsorbed intermediate is coordinated are indicated in the upper right corner of each spectra. Atom colors: O-red, Al-grey, H-green, Na-yellow, C-dark blue.

Supplementary Note: Optimized structures of adsorbed CH_3COO* and HCOO* intermediates, binding energies, and vibrational wavenumbers on hydrated γ-Al_2O_3 surfaces and the Na-modified hydrated γ-Al_2O_3 surfaces are reported in **Tables S5** and **S6**, respectively. The corresponding computed vibrational spectra are depicted in **Figures S12** and **S13**, respectively. Formate and acetate surface intermediates on hydrated γ-Al_2O_3 surfaces prefer to bind in bidentate configurations (**Table S5**), specifically chelating bidentate on $Al_2O_3(110)_{2H2O}$ and bridged bidentate on $Al_2O_3(100)_{2H2O}$, in accordance with earlier DFT reports on other metal and metal oxide surfaces.[9–11] On the Na-modified surfaces (**Table S6**), acetate and formate prefer to bind coordinated to Al on $Na/Al_2O_3(110)_{2H2O}$ and coordinated to both Na and Al on $Na/Al_2O_3(100)_{2H2O}$. Acetates bound on the Na-modified surfaces exhibit vibrational signatures in the 1400-1500 cm^{-1} region. Chelating bidentate CH_3COO* coordinated to Al has an asymmetric OCO-stretching vibration, υ_{as}(OCO) at 1530-1520 cm^{-1}, and a prominent OCO-stretching, υ_s(OCO) at ~1460 cm^{-1} accompanied with CH_3 deformations, primarily caused by C-H bending in 1400-1500 cm^{-1} range (**Figures S12-13**). This species is most well-aligned with the 1460 cm^{-1} band observed experimentally. The adsorbed formate structures do not exhibit bands in 1400-1500 cm^{-1} region, on either facet of Al_2O_3 or Na-modified Al_2O_3.

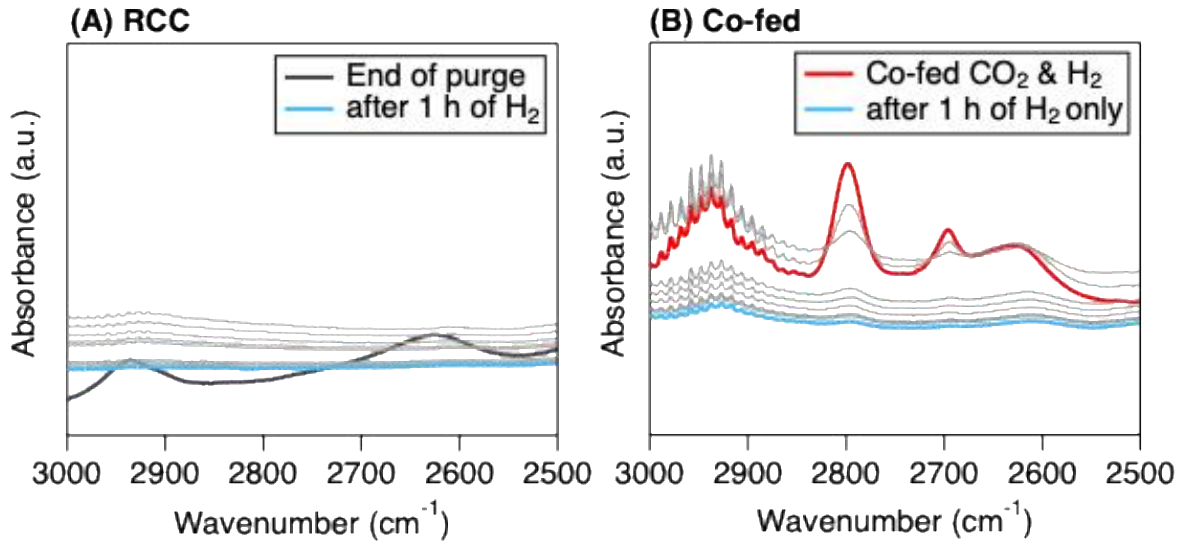

Figure S14: Comparison of *in situ* DRIFTS 3000-2500 cm^{-1} wavenumber region during (a) reactive desorption at 300°C (following CO_2 adsorption and 1 h purge in inert) and (b) co-fed hydrogenation at 300°C (CO_2:H_2 = 1:4, 10% CO_2,40% H_2, balance He) on Ru+Na/Al_2O_3.

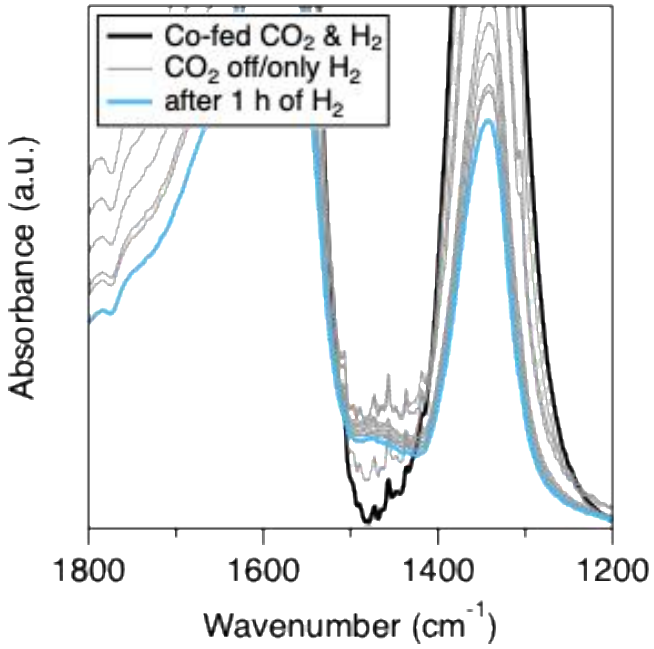

Figure S15: Zoom of 1800-1200 cm^{-1} region (corresponding to spectra shown in Figure 4) to emphasize the growth of ca. 1460 cm^{-1} peak with the shut-off of H_2 following co-fed hydrogenation over $Ru+Na/Al_2O_3$.

Supplementary Tables

Table S1: Weight loading of Alk metal (%) of Al_2O_3-supported Alk sorbents.

Material	% sorbent metal
Na/Al_2O_3	2.7
Mg/Al_2O_3	4.4
K/Al_2O_3	5.1
Ca/Al_2O_3	5.3

Supplementary Note: Elemental content of the materials was assessed through inductively coupled plasma optical emission spectroscopy (ICP-OES). Approximately 25 mg of material was added to a PTFE digestion vessel and combined with acidic solutions (8 mL concentrated HNO_3 for supported sorbents and 5 mL HNO_3 and 3 mL HCl for DFMs). The vessel was loaded into a microwave digestion chamber (Ultrawave) and heated for 1 h at 250 °C under a nitrogen pressure of 40 bar. Following digestion, each solution was diluted to 50 mL with DI water. A 5 mL aliquot was then taken and further diluted to 50 mL in a 14% HNO_3 matrix. These dilutions were analyzed on an Agilent 5110 ICP-OES alongside standards for Al, Na, K, Mg, and Ca at 0, 5, 10, 20, 40, and 100 ppm and Pd and Ru at 0, 5, 10, and 20 ppm in the same matrix.

Table S2: Cleavage and surface energy of various terminations of the (110) and (100) surfaces of γ-Al_2O_3. Corresponding structures for each termination are depicted in **Figure S4**.

Surface Slab	Term.	Slab Dimensions (x × y)	Cleavage Energy (mJ/m^2)	Surface Energy (mJ/m^2)	O:Al
(110)-4L	T1	8.413 Å × 8.068 Å	3517.89	1763	24:16
	T2		3049.69	1589	
	T3		2541.94	**1393**	
(110)-8L	T1	8.413 Å × 8.068 Å	3553.19	1925	48:32
	T2		3074.71	1733	
	T3		2551.50 (Digne *et al.*: 2590)[1]	**1530** (Digne *et al.*: 1540)[1]	
(100)	**T1**	5.587 Å × 8.413 Å	1420.18	**960.5**	24:16
	T2		2574.67	1500.6	
	T3		3351.61	2627.2	
	T4		3996.61	3016	

Table S3: CO_2 adsorption geometries and corresponding adsorption energy (E_{ads}, in eV) and computed wavenumbers (cm^{-1}) on $Al_2O_3(110)_{2H2O}$ and $Al_2O_3(100)_{2H2O}$. Only wavenumbers above 900 cm^{-1} are reported. Atom colors: O-red, Al-grey, H-green, C-dark blue. Distances in Å

	$Al_2O_3\,(110)_{2H2O}$		$Al_2O_3\,(100)_{2H2O}$
Physisorbed CO_2	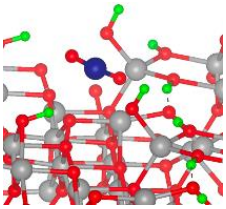 E_{ads} = -0.35 eV ν = 2362, 1311 cm^{-1}		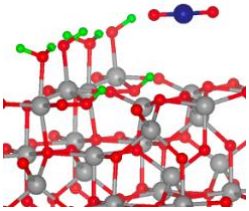 E_{ads} = -0.1 eV ν = 2368, 1322 cm^{-1}
Chelating bidentate carbonate (c,b-CO_3*)	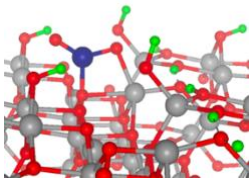 E_{ads} = -0.76 eV ν = 1812, 1160 cm^{-1}		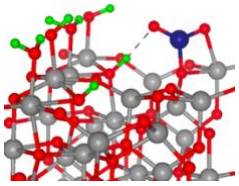 E_{ads} = -0.75 eV ν = 1717, 1244, 964 cm^{-1}
Bridged bidentate carbonate (b,b-CO_3*)	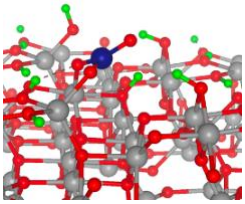 E_{ads} = -0.97 eV ν = 1687,1173,1025 cm^{-1}		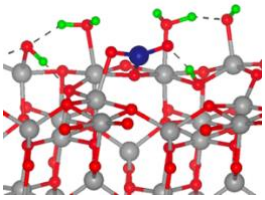 E_{ads} = -0.16 eV ν = 1690, 1244, 923 cm^{-1}
Polydentate carbonate (p-CO_3*)	**p-CO_3*(1)** 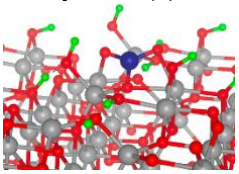 E_{ads} = -0.42 eV ν= 1632, 1248, 963 cm^{-1}	**p-CO_3*(2)** 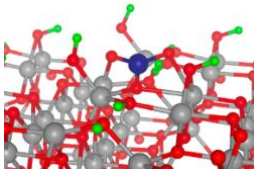 E_{ads} = -0.17 eV ν= 1523, 1372, 1070 cm^{-1}	Not identified
Bicarbonate (HCO_3*)	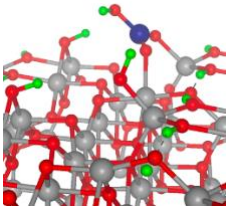 E_{ads} = -0.84 eV ν = 3687, 1633, 1421, 1207, 1049 cm^{-1}		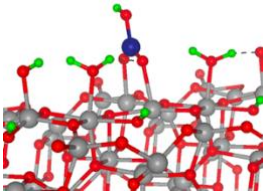 E_{ads} = -0.27 eV ν = 3679, 1633, 1385, 1198, 1008 cm^{-1}

Table S4: CO_2 adsorption geometries and corresponding adsorption energy (E_{ads}, in eV) and computed wavenumbers (cm^{-1}) on $Na/Al_2O_3(110)_{2H2O}$ and $Na/Al_2O_3(100)_{2H2O}$. Only wavenumbers above 900 cm^{-1} are reported. Atom colors: O-red, Al-grey, Na-yellow, H-green, C-dark blue.

	$Na/Al_2O_3(110)_{2H2O}$	**$Na/Al_2O_3(100)_{2H2O}$**
Physisorbed CO_2	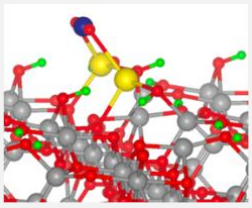 E_{ads} = -0.24 eV ν = 2372, 1319 cm^{-1}	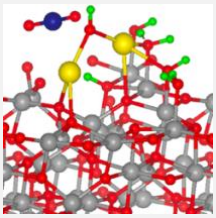 E_{ads} = -0.28 eV ν = 2339, 1301 cm^{-1}
Chelating bidentate carbonate (c,b-CO_3*)	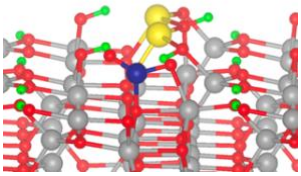 E_{ads} = -0.77 eV ν = 1805, 1159 cm^{-1}	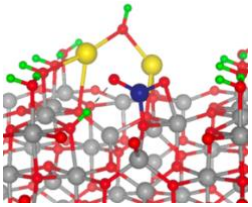 E_{ads} = -0.91 eV ν = 1672, 1239, 1011 cm^{-1}
Bridged bidentate carbonate (b,b-CO_3*)	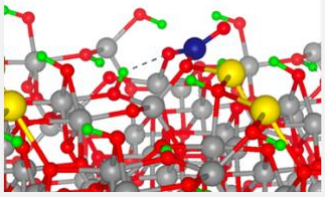 E_{ads} = -0.84 eV ν = 1656, 1190, 1026 cm^{-1}	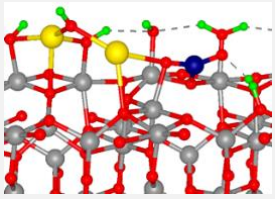 E_{ads} = -0.35 eV ν = 1647, 1230, 955 cm^{-1}
Polydentate carbonate (p-CO_3*)	**p-CO_3*(1)** 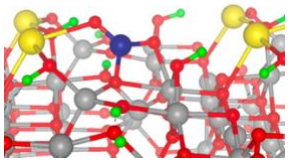 E_{ads} = -0.99 eV ν = 1728, 1238, 931 cm^{-1} **p-CO_3*(2)** 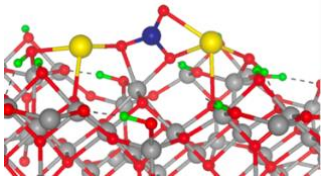 E_{ads} = -0.73 eV ν = 1660, 1268, 1001 cm^{-1}	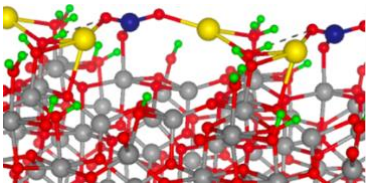 E_{ads} = -0.99 eV ν = 1545, 1285, 1004 cm^{-1}

	$Na/Al_2O_3(110)_{2H_2O}$	$Na/Al_2O_3(100)_{2H_2O}$
Bicarbonate (HCO_3*)	**HCO_3*** 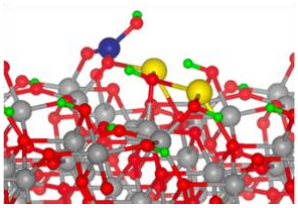 E_{ads} = -0.51 eV ν = 3690, 1640, 1390, 1197, 1029 cm^{-1}	**HCO_3*(1)** 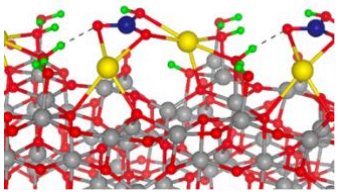 E_{ads} = -1.28 eV ν = 3710, 1657, 1318, 1168, 938 cm^{-1} **HCO_3*(2)** 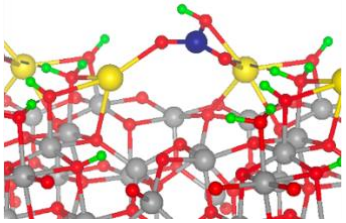 E_{ads} = -1.12 eV ν = 3713, 1719, 1290, 1154 cm^{-1} **HCO_3*(3)** 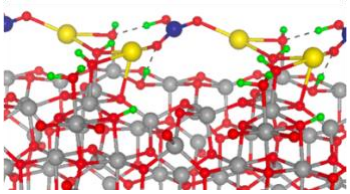 E_{ads} = -0.87 eV ν = 3182, 1668, 1353, 1300, 995 cm^{-1} **HCO_3*(4)** 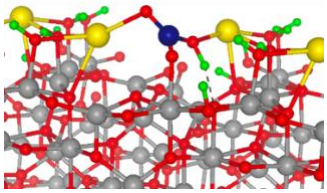 E_{ads} = -1.2 eV ν = 2890, 1697, 1432, 1255, 980, 928 cm^{-1}

Table S5: Acetate and formate adsorption geometries and corresponding adsorption energy (E_{ads}, in eV), and computed wavenumbers (cm^{-1}) on $Al_2O_3(110)_{2H2O}$ and $Al_2O_3(100)_{2H2O}$. Only wavenumbers above 900 cm^{-1} are reported. Atom colors: O-red, Al-grey, H-green, C-dark blue.

	Acetate (CH_3COO*)	**Formate ($HCOO$*)**
$Al_2O_3(110)_{2H2O}$	**Monodentate** 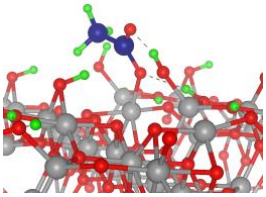 E_{ads} = -1.63 eV ν = 3102, 3052, 2983, 1575, 1426, 1412, 1322, 1282, 1019, 998, 909 cm^{-1}	**Monodentate** 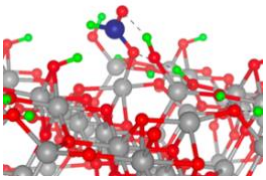 E_{ads} = -1.86 eV ν = 2910, 1609, 1327, 1233, 995 cm^{-1}
	Chelating bidentate 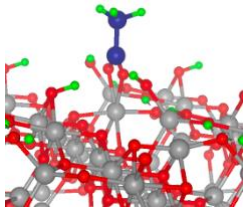 E_{ads} = -1.97 eV ν = 3102, 3062, 2989, 1520, 1468, 1421, 1406, 1333, 1025, 994, 947 cm^{-1}	**Chelating bidentate** 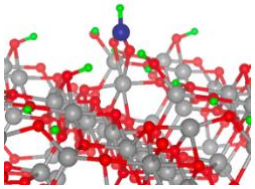 E_{ads} = -2.11 eV ν = 3000, 1552, 1365, 1278, 1005 cm^{-1}
$Al_2O_3(100)_{2H2O}$	**Bridged bidentate** 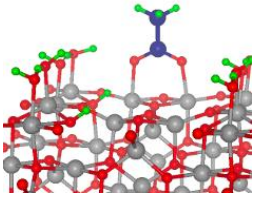 E_{ads} = -1.18 eV ν = 3105, 3063, 2989, 1532, 1436, 1411, 1386, 1326, 1019, 1003, 924 cm^{-1}	**Bridged bidentate** 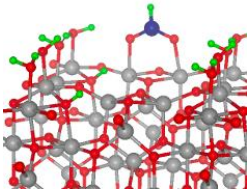 E_{ads} = -1.40 eV ν = 2950, 1560, 1362, 1322, 1001 cm^{-1}

Table S6: Acetate and formate adsorption geometries and corresponding adsorption energy (E_{ads}, in eV), and computed wavenumbers (cm^{-1}) on $Na/Al_2O_3(110)_{2H2O}$ and $Na/Al_2O_3(100)_{2H2O}$. Only wavenumbers above 900 cm^{-1} are reported. Atom colors: O-red, Al-grey, H-green, C-dark blue, Na-yellow.

	Acetate (CH_3COO*)	**Formate ($HCOO$*)**
$Na/Al_2O_3(110)_{2H2O}$	**Na-coordinated** 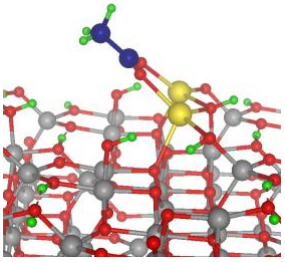 E_{ads} = -1.29 eV ν = 3078, 3054, 2980, 1448, 1423, 1413, 1385, 1323, 1018, 968 cm^{-1}	**Na-coordinated** 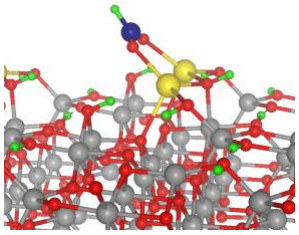 E_{ads} = -1.45 eV ν = 2719, 1515, 1271, 1150, 958 cm^{-1}
	Al-coordinated 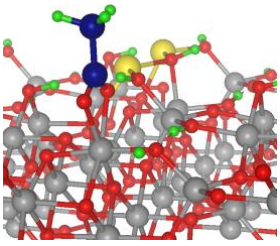 E_{ads} = -1.99 eV ν = 3093, 3060, 2990, 1530, 1462, 1425, 1407, 1329, 1027, 992, 939 cm^{-1}	**Al-coordinated** 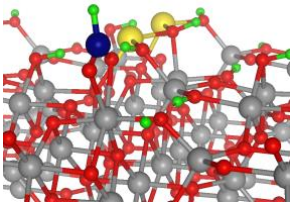 E_{ads} = -2.16 eV ν = 2984, 1560, 1363, 1280, 1001 cm^{-1}
	Na- and Al-coordinated 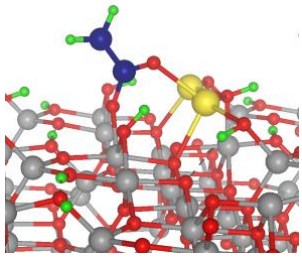 E_{ads} = -1.56 eV ν = 3094, 3047, 2982, 1566, 1430, 1415, 1381, 1316, 1019, 994 cm^{-1}	**Na- and Al-coordinated** 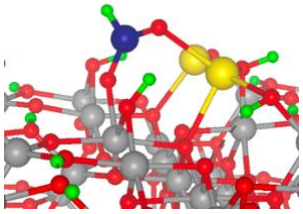 E_{ads} = -1.81 eV ν = 2872, 1600, 1349, 1337, 1014 cm^{-1}

	Acetate (CH_3COO^*)	Formate ($HCOO^*$)
$Na/Al_2O_3(100)_{2H_2O}$	**Na-coordinated** 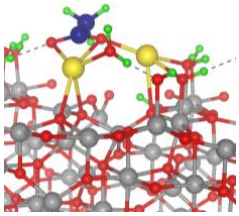 E_{ads} = -1.63 eV ν = 3083, 3048, 2970, 1492, 1433, 1414, 1392, 1320, 1022, 991 cm^{-1}	**Na-coordinated** 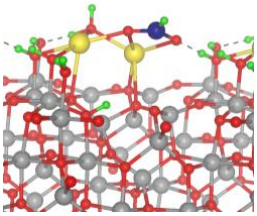 E_{ads} = -1.87 eV ν = 2865, 1568, 1344, 1328, 1013 cm^{-1}
	Al-coordinated 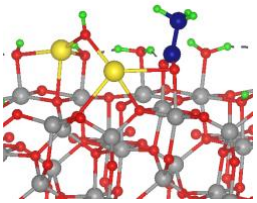 E_{ads} = -1.34 eV ν = 3100, 3058, 2981, 1518, 1433, 1409, 1387, 1324, 1027, 1000, 915 cm^{-1}	**Al-coordinated** 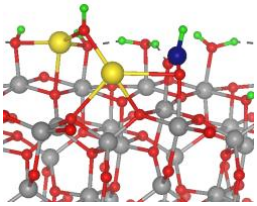 E_{ads} = -1.57 eV ν = 2918, 1545, 1360, 1321, 1006 cm^{-1}
	Na- and Al-coordinated 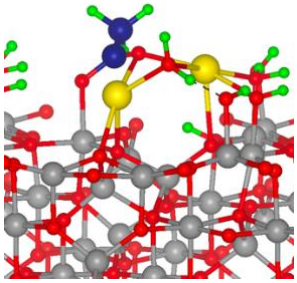 E_{ads} = -1.80 eV ν = 3093, 3047, 2980, 1568, 1421, 1412, 1367, 1309, 1029, 996, 918 cm^{-1}	**Na- and Al-coordinated** 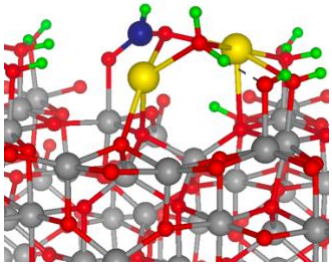 E_{ads} = -1.98 eV ν = 2904, 1583, 1354, 1322, 1024 cm^{-1}

Table S7: Structure and electronic energy of gas-phase species. Bond distances in angstrom (Å) and angles in degree (°). Atom colors: O-red, H-green, C- dark blue

	H_2O	CO_2	HCOO radical	CH_3COO radical
Structure	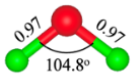	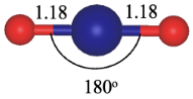	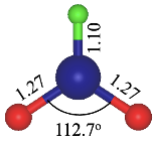	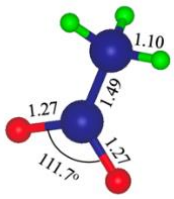
E^{DFT} **(eV)**	-14.218	-22.953	-24.048 (1 unpaired electron)	-41.071 (1 unpaired electron)

Table S8: Vibrational scaling factor (c) calculated for CO_2 by comparing experimental (ϑ_i) and DFT computed (υ_i) wavenumbers (cm^{-1}). Experimental CO_2 values obtained from NIST Computational Chemistry Comparison and Benchmark Database.[12]

ϑ_i (experimental, cm^{-1})	υ_i (PBE computed, cm^{-1})
2349	2365.74
1333	1316.99
667	632.75
667	632.69
Scaling factor, $c = \frac{\sum \vartheta_i . \upsilon_i}{\sum \upsilon_i^2}$	1.003

Supplementary References

1. Digne, M. Use of DFT to achieve a rational understanding of acid?basic properties of ?-alumina surfaces. *Journal of Catalysis* **226**, 54–68 (2004).
2. Krokidis, X. *et al.* Theoretical Study of the Dehydration Process of Boehmite to γ-Alumina. *J. Phys. Chem. B* **105**, 5121–5130 (2001).
3. Wischert, R., Laurent, P., Copéret, C., Delbecq, F. & Sautet, P. γ-Alumina: The Essential and Unexpected Role of Water for the Structure, Stability, and Reactivity of "Defect" Sites. *J. Am. Chem. Soc.* **134**, 14430–14449 (2012).
4. Weilach, C., Spiel, C., Föttinger, K. & Rupprechter, G. Carbonate formation on Al2O3 thin film model catalyst supports. *Surface Science* **605**, 1503–1509 (2011).
5. Busca, G. & Lorenzelli, V. Infrared spectroscopic identification of species arising from reactive adsorption of carbon oxides on metal oxide surfaces. *Materials Chemistry* **7**, 89–126 (1982).
6. Gruene, P., Belova, A. G., Yegulalp, T. M., Farrauto, R. J. & Castaldi, M. J. Dispersed Calcium Oxide as a Reversible and Efficient CO_2 −Sorbent at Intermediate Temperatures. *Ind. Eng. Chem. Res.* **50**, 4042–4049 (2011).
7. Schreiter, N., Kirchner, J. & Kureti, S. A DRIFTS and TPD study on the methanation of CO2 on Ni/Al2O3 catalyst. *Catalysis Communications* **140**, 105988 (2020).
8. Pan, Y., Liu, C. & Ge, Q. Adsorption and Protonation of CO_2 on Partially Hydroxylated γ-Al_2O_3 Surfaces: A Density Functional Theory Study. *Langmuir* **24**, 12410–12419 (2008).
9. Calatayud, M., Collins, S. E., Baltanás, M. A. & Bonivardi, A. L. Stability of formate species on β-Ga2O3. *Phys. Chem. Chem. Phys.* **11**, 1397 (2009).
10. Hofman, M. S. *et al.* Acetic Acid Adsorption and Reactions on Ni(110). *Langmuir* **36**, 8705–8715 (2020).
11. Gao, M., Zhang, J., Zhu, P., Liu, X. & Zheng, Z. Unveiling the origin of alkali metal promotion in CO2 methanation over Ru/ZrO2. *Applied Catalysis B: Environmental* **314**, 121476 (2022).
12. Russell D. Johnson III. NIST Computational Chemistry Comparison and Benchmark Database, NIST Standard Reference Database Number 101. https://doi.org/10.18434/T47C7Z (2022).